Available online at www.sciencedirect.com
SCIENCE DIRECT®
Physica A 325 (2003) 297–318
PHYSICA A
www.elsevier.com/locate/physa

Force–displacement distributions and percolation properties in simulated 2-D packings

A.M. Vidales[a,*], I. Ippolito[b], C. Moukarzel[c]

[a] *Departamento de Física y CONICET, Universidad Nacional de San Luis. Chacabuco 917, 5700 San Luis, Argentina*
[b] *Groupe Matière Condensée et Matériaux (UMR CNRS 6626), Université de Rennes 1, Bât 11A, Campus de Beaulieu, 35042 Rennes Cedex, France*
[c] *Departamento de Física Aplicada, CINVESTAV, 97310 Mérida, Yucatán, Mexico*

Received 5 August 2002

Abstract

The first part of this paper studies the behavior of contact force distributions and displacement distributions in isostatic 2-D arrays of polydispersed grains as a function of force strength and displacement strength, respectively. The array is built by pouring disks, one by one, into a rectangular die. After the array is ready, force and displacement measurements are performed on it. We also introduce a relaxation procedure (rearrangements of disks) in order to study the behavior of the corresponding distributions as a function of the number of relaxations performed on the system.

In the second part, we characterize the percolation of small particles through this 2-D packings as a function of the polydispersivity of the disks. We analyze both trapping and non-trapping regimes. Characteristic features of these packings are discussed.

PACS: 45.70.Ht; 60.60.Ht; 05.70.−a

Keywords: Granular packings; Percolation; Stress distributions

1. Introduction

Characterizing solid particles packings has attracted the attention of much scientific research in the last decade [1]. Its importance is due to the wide number of technological problems related to many industrial fields, from pharmacy to civil engineering

* Corresponding author. Fax: +54-2652-425109.
E-mail address: avidales@unsl.edu.ar (A.M. Vidales).

0378-4371/03/$ - see front matter
doi:10.1016/S0378-4371(03)00140-7

and all the range you may imagine in between. For instance, the final density obtained upon a sintering process in ceramics depends critically on the initial packing fraction of the grain ensemble [2–5]; the success in mixing grains of very different sizes depends on how the small particles percolate through the big ones [6–11]. In the last years, computer simulations of packings of disks and spheres in two and three dimensions, respectively, have helped to reveal some of the important aspects of granular systems, as cited below.

In this work, we perform simulations of granular packings in 2-D by throwing disks into a die to represent the actual experiment of poured grains into a rectangular container until it is completely full. This simulated experiment will allow to measure some basic quantities that characterize this kind of assemblies: distributions of contact force between grains, distribution of displacements when you slightly perturb the system and percolation properties related to the passage of small grains compared to the ones conforming the pack. There have been previous works where this kind of packings have been generated [12–14]. Typically, the calculated geometrical properties were density, average number of contacts, radial distributions and size distribution of interstices. There has been a number of works trying to elucidate the behavior of the force distribution above and below the mean force value [2,12–25]. Most of them deal with monosized or uniform radii distributions and a complete justification of the behavior found is still difficult to provide. Other kinds of radii distributions and uniform distributions with varying parameters have not yet been employed to our knowledge.

Iter-particle percolation is defined as the drainage of small particles through the interstices between large ones. This phenomenon takes place in failure zones of higher porosity than the bulk. It can be induced by shear [7,8] or occur spontaneously under gravity [9,10], if the diameter of the percolating particles is sufficiently small compared to that of the packing particles.

In previous works, Bridgwater et al. [6–10] and Ippolito et al. [11] have studied spontaneous percolation inside beds of glass beads. The first authors studied essentially the variations of the diffusive properties of the motion as a function of the restitution coefficient and the second ones analyze the dispersion coefficients parallel and transverse to the mean velocity by studying the bead distribution at the exit (XY plane) and the transit time distribution as the height of the packing is changed. Diffusion in both directions was found to depend essentially on the diameter of packed spheres and not by the size of the small percolating beads.

In what follows, we will present our results on 2-D grain packings. Firstly, we will refer to numerical results concerning the behavior of contact forces network and displacements for packings with uniform radii distributions. Forces and displacements distributions are measured using the fact that our systems present isostatic properties. We will prove that the behavior found for contact force distributions is in agreement with previous evidence related to packings where no restriction on the sign of the forces is imposed [25].

Secondly, we will present numerical results characterizing the percolative–non-percolative regimes and the transition in between, for the diffusion of small particles through the packings. We will draw interesting results mainly related to the entrapment regime that, other wise, cannot yet be obtained experimentally.

2. Numerical generation of the grain packing

The computer algorithm used in the present simulations has been programmed in a way that allows to generate packings of disks sampled from any desired size distribution. The time needed to set a packing of 10,000 disks and to obtain all the quantities of interest is just a few seconds on a Pentium III PC.

First, a radii distribution for the disks is selected and 10,000 disks are randomly sampled from it. Then, the bottom of the packing is built by first putting $N = 30$ disks of randomly selected radii, side by side and fixing the walls until touching the two extremes. This value ensures a convenient ratio height over width to measure the desired distributions. In this way we fix the width of the die. After that, the remaining disks are pouring one at a time from the top of the die, selecting at random their horizontal position and keeping them from overlapping the walls of the container. Each grain falls down following a steepest descent algorithm. Once it touches already deposited disks, it rolls over them until a stable position is found. By stable position we mean the first time the center of the falling particle is in between the center of the two first particles it touches. In the case a stable position is attained where one of the contacting disks has a vertical coordinate for its center that is greater than the corresponding one for the new disk, a bridge position is defined and counted. Side walls are consider without friction.

Once all the particles are deposited in the die, a relaxation process is carried out by using an algorithm to mimic the effect of a large-amplitude, low-frequency vertical shaking [23]. This process is executed in order to attain static equilibrium throughout the system and to study its influence on the force–displacement distributions and one of the main consequences of it, as discussed below, is to reduce the number of bridges between grains [26]. This "shaking" algorithm is defined as follows. Particles are allowed to fall down again into the die, one at a time (the bottom is conserved). The first to fall is the one whose center has the lowest vertical position in the previous packing configuration, then, the next whose vertical position is the lowest, and so on. Rules to attain equilibrium are the same as before. After an order of 10 relaxations, we observed that the configuration of contacts and the strength of forces or displacements did not change any more. In the next section, we will analyze the effect of bridges in force and displacement distributions.

The disks assemblies used to study percolation properties were built in the same way as above, but no further compaction (relaxations) were done in this case after the array was completed. Then, the position of the center of the disks is kept fixed for the rest of the percolation process. For these packings N was chosen equal to 100 to ensure that the percolating particles do not collide with the die walls (see below).

3. Contact force and displacement distributions

3.1. Contact Forces

To measure force and displacement distributions we employed uniform radii size distributions centered at 1 a.u. (arbitrary units) with a fixed dispersion of 10%,

assuming the same weight for all the grains, no matter its size. As discussed above, because of the deposition rules used, each new particle added to the packing will create two new contacts to achieve its static equilibrium. Thus, the system will be isostatic. It has been shown [21,22] that disordered packings of frictionless, cohesionless granular materials, idealized as spheres, have, in any dimension d, an isostatic contact network for small or null external pressure compared to the stiffness of the grains. Our results show that our packings are isostatic with a mean coordination number of four contacts [26]. Isostaticity is an important property to take into account when contact forces and displacements have to be calculated. An isostatic ensemble of grains makes it possible to state Newton's equations for force balance straightforwardly because forces are determined by local conditions [21,22]. One can solve the system starting from the last deposited grain and going on through the next grains following their time sequence deposition. Thus, when the grains at the bottom of the die are reached, all forces are already known. This means that only the equilibrium equation is enough to solve all the equation system by propagation.

All forces are considered central and no rotations are allowed. It is expected that, no matter the weight assumption, negative forces will appear when the force equations are solved [25]. The deposition procedure produces isostatic lattices, but has no built-in sign constraint for stresses, therefore, tensile stresses may appear.

We also measured the displacements D_{ib} induced in site i when bond b is stretched. It has been shown in Ref. [25] that these displacements correspond to the force–force Green functions of the system. After the packing has been built and its contact forces calculated, a randomly chosen particle in the bottom layer is shifted vertically. The size of the displacement is not relevant since our system is linear in the limit of large stiffness. The new equilibrium positions are calculated easily by upwards propagation, given the system is isostatic. A deformation of the type described here does not modify the repose length or stress of any of the bonds in the system, thus, the sole condition that bond lengths be constant is enough to find how much the upper particles are displaced, knowing how much the lower particle is displaced.

In Fig. 1(a) we show the results for force distributions $P(f)$ averaged over 10^5 equivalent packings. These distributions were calculated for the first arrangement obtained after the last particle was poured into the die, i.e., no further relaxation (shaking) was done on the system. Data are plotted in six sets according to the depth of the particles exerting them, i.e., we divided the total height of the system in six bands at different heights and made statistics in each one. Forces of both signs appear but in this figure we only plot the positive ones. The distributions $P(f)$ are approximately symmetric around zero. They show a power law behavior for large strengths. This is not in contradiction with previous results regarding the existence of an exponential decay of $P(f)$ for large forces [25]. This last behavior is expected when restrictions are imposed over the sign of the forces, avoiding the presence of negative ones (tensile stresses). This has been investigated in different ways by several authors [25,27,28]. But here, both types of forces are allowed, tensile and compressive ones. Unlike for the case of just compressive forces, here the cutoff in $P(f)$ grows exponentially with depth as seen in the same figure.

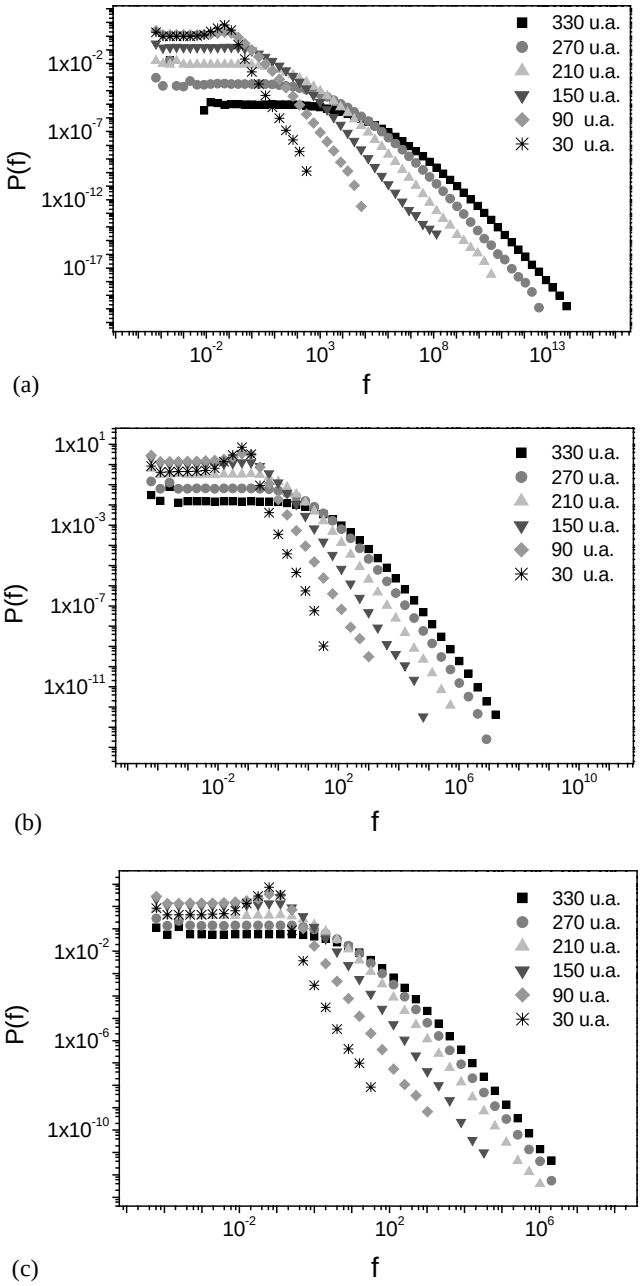

Fig. 1. Normalized contact forces after different number of shakings; (a) before any relaxation; (b) after five relaxations; (c) after 10 relaxations. Note the change in scale as relaxations go further.

In Fig. 1(b) and (c) we plot the behavior of the normalized contact forces as we relax the system a certain number of shakings. Part (b) shows distributions after five relaxations and (c) after 10. This relaxing is the one depicted above. As can be seen, this process clearly affects the quantitative behavior of the distributions, but they still remain qualitatively the same. For all depths, the strength of large forces decreases considerably after the first five shakings, while for small forces, the probability of occurrence tends to equal each other, as seen in Fig. 1(b).

The behavior for even more relaxations (Fig. 1(c)) is practically the same and, as said above, a stationary state is attained after this number of rearrangements. It seems that low-frequency, high-amplitude shakings help the grains to order in such a way that their contacts support smaller stresses. We presume that one reason for this curious behavior is the decrease of the number of bridges, enhancing the stability of the packing and lowering the presence of contacts altering the propagation of stresses downwards. In fact, when a new particle is added to the die, it may happen that one of its two contacts in its stable position forms what we define as a bridge. We will say that a bridge is present when one of the contacts supporting the particle forms any angle *above* the horizontal. This local configuration will not propagate stresses in the same way like the standard one where the two contacts are *below* the horizontal. We may say that the presence of a bridge alters the propagation of stresses downwards, given the fact that one of the supporting contacts is really lacking.

3.2. Displacement distributions

Concerning displacements, the corresponding normalized distributions $P(D)$ are shown in Fig. 2 for different relaxation stages that correspond with those in Fig. 1. They are classified in nine sets according to the depth of the particles suffering a displacement D. Our numerical results show that $P(D)$ has a broad distribution with power law behavior for D smaller than a cutoff value and this cutoff grows exponentially with the distance to the bottom (remember the picture here is opposite to the case of forces). As argued in Ref. [25], on general isostatic networks, this power law behavior for displacements is expected no matter whether sign restrictions are present for stresses. As for $P(f)$, relaxations produce a decrease in the magnitude of displacements whatever the depth is. Comparison of Figs. 2(a) and (c) shows a decrease of 8 orders of magnitude after 10 shakings. Nevertheless, the qualitative behavior of the distributions is not affected.

We also investigated whether $P(f)$ and $P(D)$ would behave in the same way as reported in Ref. [25] for a packing of monosized disks generated in the way explained above. In Figs. 3 and 4, we plot the corresponding distributions and also show how shakings affect them. The radii distribution of the disks in these packings has a delta shape with its peak at 1 a.u. and a narrow dispersion of 1%. The same die and number of particles were used here than above. As seen in part (a) of the two figures, we recover the same behavior from as in Ref. [25]. Moreover, and according to our expectations, the relaxation process effect is lesser in both distributions, given the fact that disks form a practically ordered array without too much opportunities for bridges to develop (see parts (b) and (c) of Figs. 3 and 4). It is worthy to mention that, here,

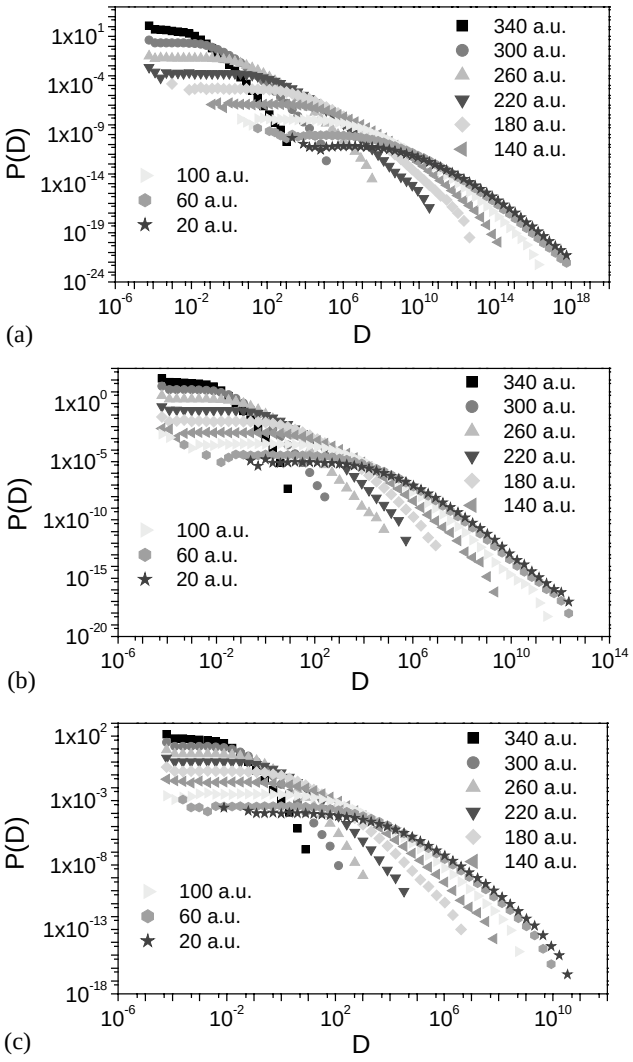

Fig. 2. (a–c) Normalized displacement distributions $P(D)$ for three different relaxation stages that correspond to the same ones of Fig. 1. They are classified in nine sets according to the depth of the particles suffering a displacement D. Here depth is also measured in arbitrary units as indicated.

the larger forces are about 5 orders of magnitude smaller than their counterparts for disordered packings. This shows the effect of disorder in stress propagation and also reinforce our argument on the importance, in this sense, of the presence of bridges. The same observation can be done for $P(D)$ concerning the strength of displacements.

Finally, Fig. 5 shows the second moment of $P(f)$. In part (a), we plot it for uniform distributions and in part (b) for monosized ones. For both distributions, this

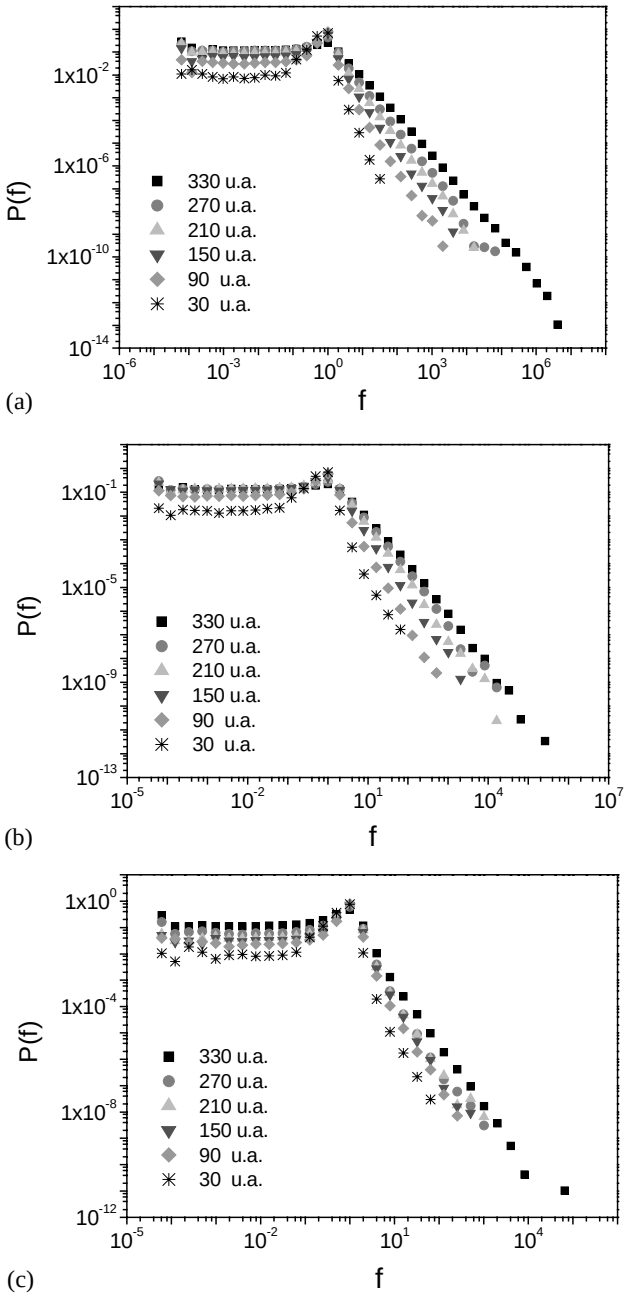

Fig. 3. Normalized contact forces distributions $P(f)$ for a packing of monosized disks. (a) before any relaxation; (b) after five relaxations; (c) after 10 relaxations. Compare the effects of shakings with Fig. 1.

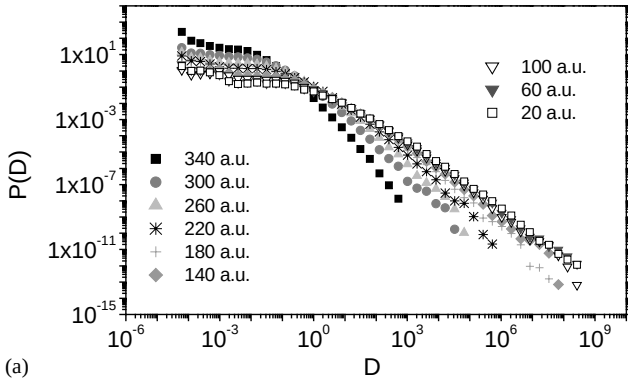

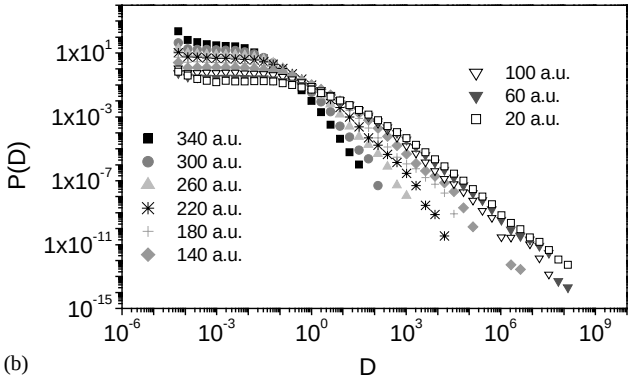

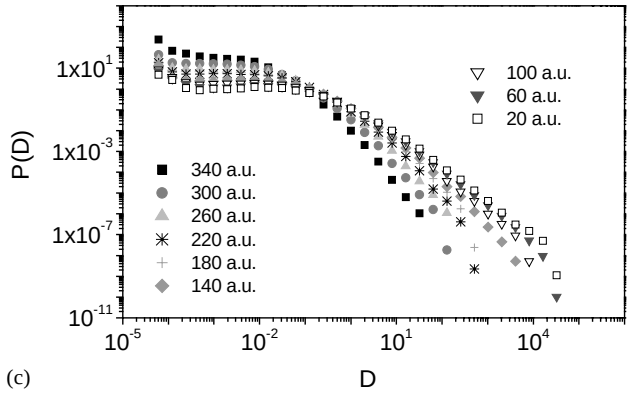

Fig. 4. (a–c) Normalized displacement distributions $P(D)$ for a packing of monosized disks. The classification and relaxation stages are the same as in Fig. 2.

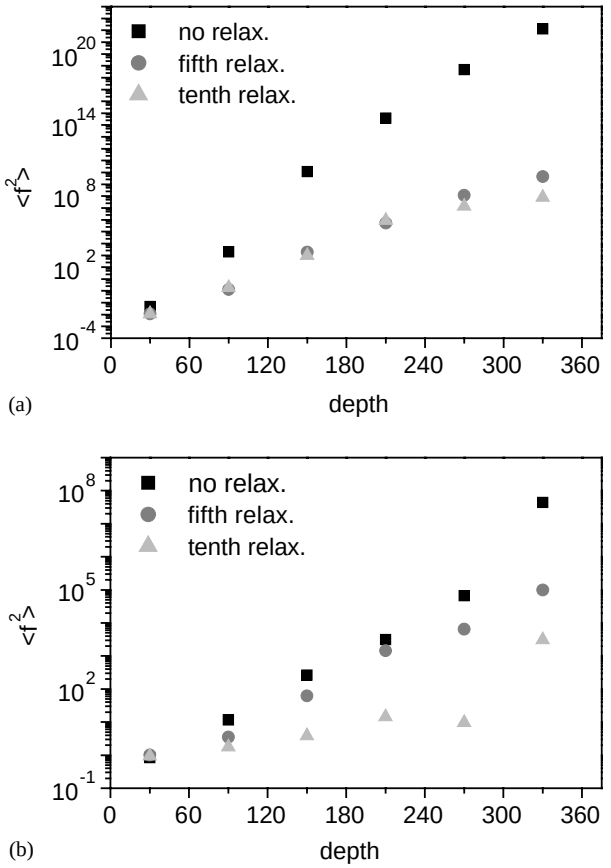

Fig. 5. Second moment in $P(f)$ (a) uniform distribution; (b) monosized distribution.

moment grows exponentially with depth and, again, the relaxation process produces an interesting effect. The slopes of the lines (representing a least-squares fitting of the simulation data) decrease as the number of shakings increases. The second moment in $P(D)$ presents the same behavior depicted for $P(f)$.

4. Percolation study

We want to simulate the percolation of a small particle through our 2D packings of grains. We generate the packings as depicted in Section 2. Suppose the die belongs to the XY plane. The radii of the disks are randomly sampled from a Gaussian density distribution. Remember that no further relaxation is done in this case and the position of the center of the disks is kept fixed for the rest of the percolation process.

Once the packing is ready and in order to create empty space for allowing the small particle to move into it, a shrinking process on the radii is started, i.e., each disk radius, R_i, is replaced by bR_i, where $b \in (0,1)$ and is the same for all R_i, i.e., the shape of the radii distribution is unchanged.

After the shrinking process is performed, the small particle is launched from above. Its initial X position can conveniently be randomly chosen or it can be fixed at any place. During the falling down, their successive positions are recorded each time a collision with a disk occurs. Its final XY position is also registered, either for the case of percolation or trapping. Statistic over a great number of equivalent samples is performed.

First, we will present general results concerning the non-capture/capture regime and main features of the little particle moving process. We will analyze the percolative–non-percolative transition through a detailed study of the mean square deviations of the exit and trapping spatial distribution histograms.

Second, we will concentrate ourselves in describing the trapped region process, given the fact that this region cannot be yet studied using experiments. Thus, these are the cases where simulations can bring light to better understand the percolating process.

4.1. General features of the percolative process

Suppose we have a packing of disks whose radii are randomly sampled from a Gaussian distribution of mean R_m and dispersion σ, truncating its width to 4σ, i.e., the extreme possible values for the radii of the disks are $R_{\max} = R_m + 2\sigma$ and $R_{\min} = R_m - 2\sigma$. The small percolating particle has a radius R_p.

To study the behavior of the diffusing process through the packing, we first have to determine b_c, which is the critical value for b in the shrinking process explained above. This means that, when all the radii of the disks are multiplied (reduced) by this b value, enough empty space is generated for the small particle to percolate though the interstices.

This critical value will depend on the radii distribution parameters and on R_p. Thus, we fixed the mean of the gaussians to $R_m = 2$ arbitrary units (a.u.) and the radius $R_p = 0.2$ a.u. and keep this values fixed for the rest of our study. Then, we determine the percolation threshold b_c for different values of σ. To this end, a standard percolation threshold searching procedure was used. Statistics over 10^3 equivalent samples with the same parameters were done, launching the small particle from randomly initial X positions. The results for b_c versus σ are shown in Fig. 6. As expected, the limiting value for a monosized distribution ($\sigma = 0$) is $b_c = b_0 = 1 - f$, where $f = R_p/R_m$. Here, we have $f = 0.1$, thus, $b_0 = 0.9$.

As the dispersion increases, percolation is hampered and b_c has to decrease in order to generate more empty space. This means that a wide radii distribution needs to offer a less dense configuration for the small particle to percolate. This can be easily explained as follows. When a distribution has a small dispersion, disks build arrays that have a higher degree of order than those for wider ones. Consequently, spaces between particles have a typical size and the shrinking process creates voids homogeneously. When the dispersion increases, the probability that small disks occupy the

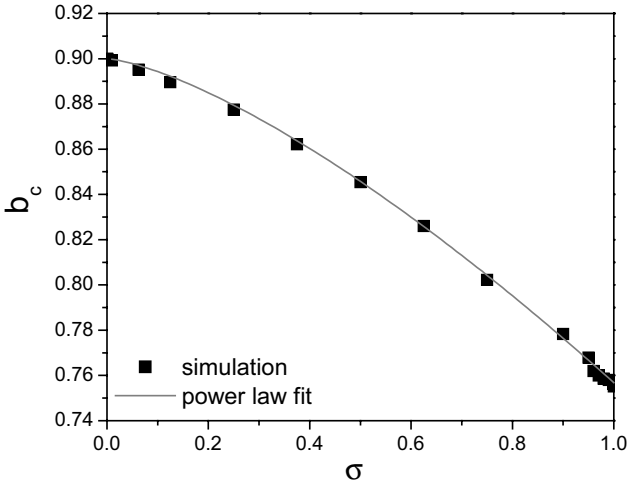

Fig. 6. Percolation thresholds, b_c, as a function of the dispersion of packed grains.

spaces between big ones increases. Then, the sizes of the paths for the percolating particle are smaller and this fact controls the shrinking process, giving smaller values for b_c.

Data on this figure can be fitted best with a power law function given by

$$b_c = 0.9 - 0.1432\sigma^{1.4} . \tag{1}$$

This equation can be rearranged in this way:

$$\frac{b_0 - b_c}{b_0 - b_l} = \sigma^{1.4} , \tag{2}$$

where b_l is the limiting value for b_c when $\sigma \to 1$. Thus, the ratio of the departure of b_c from its limiting values follows a simple power law of the mean deviation.

To our knowledge, this is the first time that the dependence of a granular percolation parameter (b_c) is found as a function of a packing distribution parameter (σ) and the power law dependence is not surprising given the critical transition studied here.

4.2. Trapping transition

Once the thresholds were determined, we took, as a first insight, the particular case $\sigma = 0.5$ to study the behavior of the percolating particle below, around and above the percolation threshold. For this case, $b_c = 0.8455$.

Fig. 7 presents the results for the exit distribution frequency as a function of final X_p (transversal coordinate of the particle). It is worthy to say that, in this set of data, the launching point of the small particle is fixed at the middle top of the die. If the particles are in the percolation regime, X_p is their final x-position at the exit. If the particles are in the entrapment regime, X_p represents its final x-position, no matter their final y-position. In (a), the b values selected are above the threshold b_c, corresponding

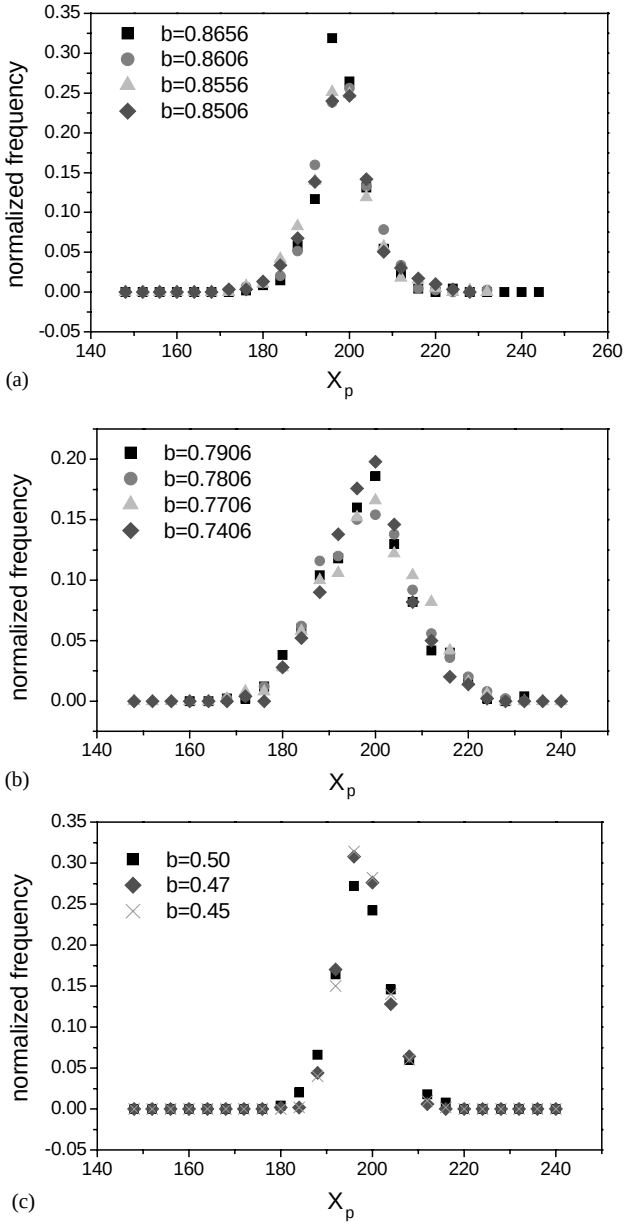

Fig. 7. Exit distribution frequencies as functions of final X_p (transversal coordinate of the particle). (a) Selected b values are above the threshold b_c (non percolative regime); (b) and (c) correspond to the distributions for b close to b_c and for b far below b_c, respectively.

to the non percolative regime. Thus, the results are the final X_p coordinates of the entrapped particles.

Parts (b) and (c) correspond to the distributions for b close to b_c and b far below b_c, respectively. As observed, the shape of the distributions are Gaussian-like. The dispersion in X_p is wider when b is closer to b_c. As b decreases, the increment of the void space between particles makes the diffusive process less disperse. This behavior resembles the one found in Galton boards [29]. All results are averaged over 10^3 equivalent samples.

From this first results, we conclude that a detailed study of this transition from one regime to the other is quite relevant. The key questions to answer are whether the Gaussian behavior for the exit distributions is maintained for different radii distributions of the packed particles and what is the behavior of the exit dispersion around b_c.

To this end, we performed two sets of simulations for extreme values of the packed particles dispersion σ. They were $\sigma = 0.01$ (almost monosized grains) and $\sigma = 0.09$ (highly polydispersivity).

For each σ value we record the exit distributions for the final X_p, like above, for several values of b close to b_c. Each distribution was then fitted with the theoretical function that resulted the best one for this purpose. The dispersion, w, corresponding to each fitting function was then plotted against b. It is important to point out here that no misunderstanding should be done among the dispersion σ of the packing particles and the dispersion w of the exit distributions. We found a clear transition in w as b goes through b_c for both cases (0.01 and 0.9) as is depicted below.

In Fig. 8, we present the results for the exit distributions obtained from 5×10^3 equivalent samples. They are all normalized in order to be compared.

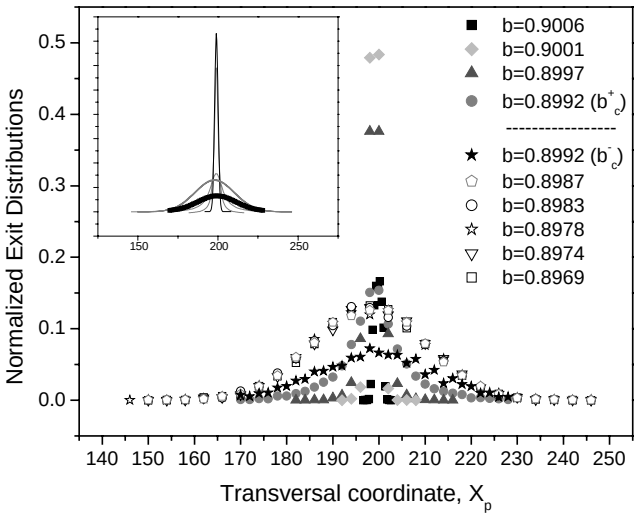

Fig. 8. Normalized exit distributions for final X_p of the percolating particle through assemblies with $\sigma = 0.01$ and for several values of b, close to b_c. Dot line serves as a guide to distinguish the percolating regime from the non percolating one.

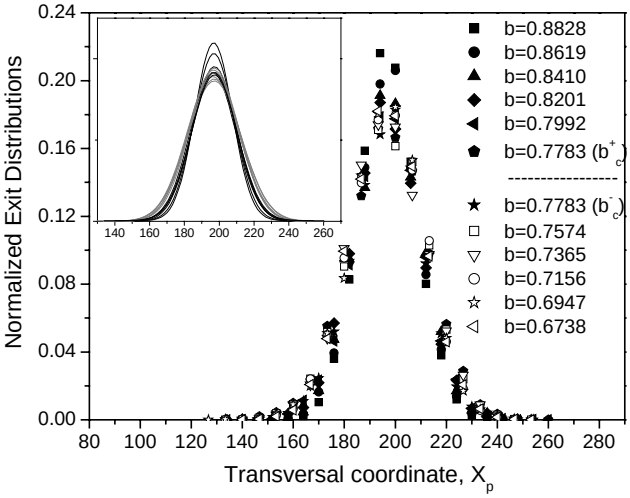

Fig. 9. Normalized exit distributions for final X_p of the percolating particle through assemblies with $\sigma = 0.9$ and for several values of b, close to b_c. Dot line serves as a guide to distinguish the percolating regime from the non percolating one.

The corresponding b values for each histogram are indicated and the dot line serves as a guide to distinguish the percolating regime from the non-percolating one. The minus and plus symbols over b_c indicate that the distribution corresponds to final X_p of trapped particles (b_c^+) and final exit X_p of percolating particles (b_c^-). This distinction is crucial because, just on b_c, the regime transition is such that not all the particles percolate, nor are completely entrapped. The inset of this figure shows the corresponding fitting functions for each case. They are all Gaussians through the percolating regime and on b_c, but a curious change occurs for b above b_c: the best fit is obtained with a Lorenzian function. This feature is explained if one takes into account the fact that the packing particles are quite monodispersed (remember $\sigma = 0.01$). As we will see in the next section, for small dispersion, the transition is abrupt and the particles soon get trapped, with almost no penetration at all. This changes appreciably the dynamics of the diffusing process that no longer belongs to a standard one. It is worthy to say that the correlation parameter obtained from all the fitting processes performed was equal to 0.99.

We show the results for exit and trapping distributions for $\sigma = 0.9$ in Fig. 9. As before, the different b values are indicated through different symbols and the dot line again separates the percolation regime from the non-percolation one. As clearly seen, all the histograms belonging to both regimes present Gaussian-like shapes. Here the inset shows the Gaussian fitting functions. In all cases, the correlation parameter R obtained from the fitting process was 0.99. The change in shape of the distributions is quite less pronounced than the corresponding to $\sigma = 0.01$. We can better appreciate this looking at Figs. 10 and 11. Comparing these two figures, we can observe that the values for dispersion below b_c are greater that their counterparts for small σ, and that

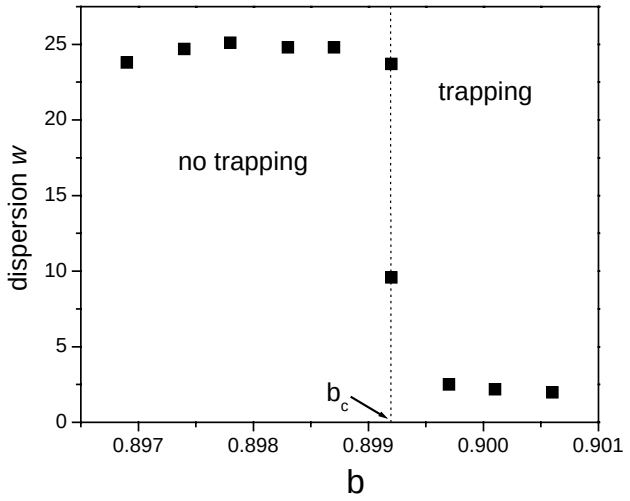

Fig. 10. Transition behavior for dispersion around b_c for $\sigma = 0.01$.

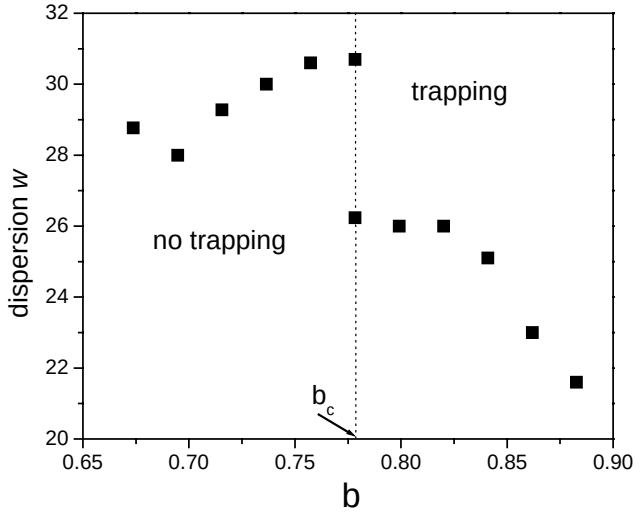

Fig. 11. Transition behavior for dispersion around b_c for $\sigma = 0.9$. Compare with Fig. 10.

the transition occurs in a wider range of b values. Another feature to point out is that, as b decreases far below b_c, dispersion also decreases. This behavior is stronger for $\sigma = 0.9$. The explanation for this different behavior is straightforward keeping in mind the order/disorder picture of the packed grains. For small σ, the grains are close to an ordered crystalline structure and the possible paths for the percolating particle are quite

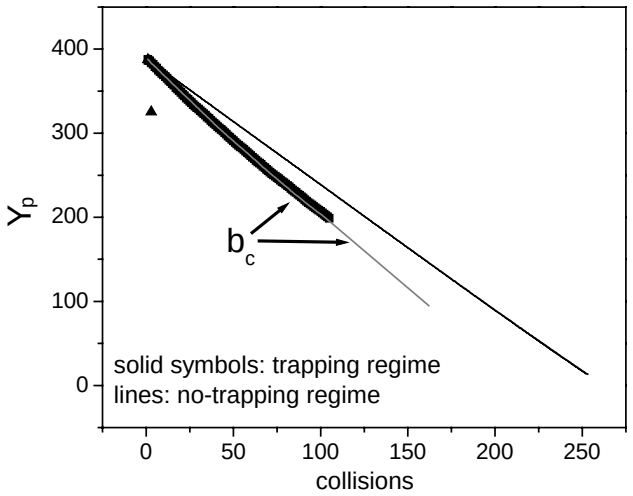

Fig. 12. Successive Y_p positions of the falling particle against cumulative number of collisions. Symbols correspond to trapping regime and all lines correspond to non-trapping behavior.

regular and similar in size. The shrinking process creates empty space in an "ordered" way. That is the reason why the transition is abrupt.

When a great polydispersion is present ($\sigma = 0.9$, for example) disorder plays a main role in smoothing the transition.

Concerning the successive Y_p positions of the falling particle, we plot the results for different b values against cumulative number of collisions in Figs. 12 and 13, for $\sigma = 0.01$ and $\sigma = 0.9$, respectively. We always found a linear behavior as can be observed. The Y_p coordinate of the particle is taken from the bottom of the die to the top of it ($Y_p = 0$ at the bottom). This linearity means that the free path traveled by the particle in the Y direction between successive collisions is the same at a given b value. We also observe that steady state regime is quickly reached after a few impacts, resembling experimental observations [11].

Concerning the slopes of the lines, we observe that for $\sigma = 0.01$, all plots for b below b_c collapse onto the same line, meaning that, once the transition occurs, the particle collision dynamics is the same. For $b = b_c$, the slopes of the lines corresponding to particles that get trapped and those which succeed to percolate are the same (see line and symbols indicated in Fig. 12). So, the transition is continuous in this sense. Above b_c, data available is difficult to analyze, given the fact that only few collisions occur before entrapment. Just two points are plotted in the figure (triangles) for $b = 0.8997$, showing an increase in slope. For $\sigma = 0.9$, we show in Fig. 13 that all lines corresponding to the non-percolating phase clearly increases their slopes as b increases, as pointed out above for $\sigma = 0.01$. This behavior can be explained taking into account the shrinking process. When b is far b_c, the only paths for the percolating particle are those created between the biggest grain (remember that empty space is proportional to $R(1 - b)$), so the tortuosity of the particle path through the packing is low and,

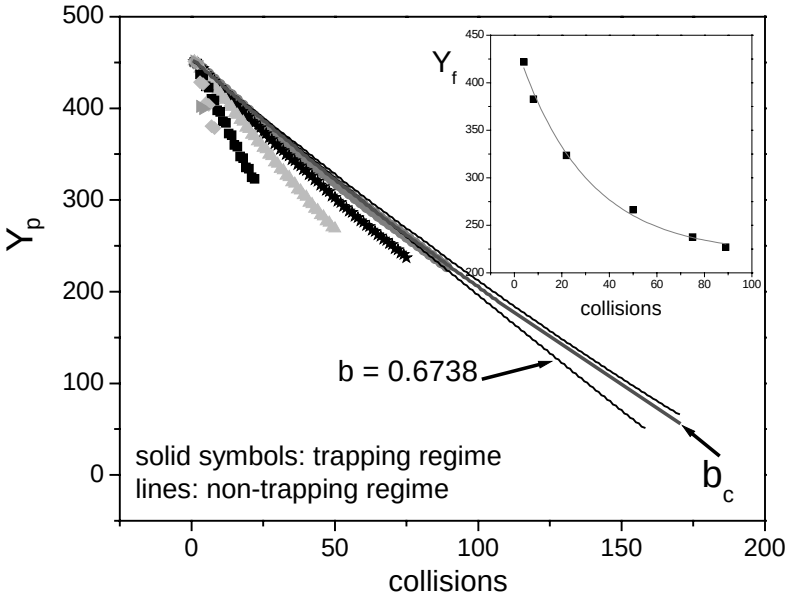

Fig. 13. Successive Y_p positions of the percolating particle vs. cumulative number of collisions. The inset just shows the penetration depth as a function of collision steps for b values above b_c (trapping regime). They follow an exponential decay as indicated by the fitting line. The thick line indicates positions for b_c.

if empty space exists, the falling is straightforward, but short. When b gets closer to b_c, more paths are created and tortuosity increases, hampering the Y displacement, but getting a deeper penetration (see the inset in Fig. 13).

For $b = b_c$, the two plots coincides like in $\sigma = 0.01$ case. They are indicated by arrows. Symbols are related to trapped particles and the thicker line correspond to percolating particles. As b goes below b_c, we observed no change in slope for b close to b_c down to $b = 0.6738$. For this last value of b, we begin to observe a change in slope. This change is due to a lower density of grains that makes the topography of the packing easier to get through it. In terms of the tortuosity view, this means that no more new paths are created and the effect of decreasing b is just to loose the packing even more.

It is worthy to point out that all the results depicted above concerning the movement of the small particle qualitatively agree with experimental observations in which respect to the percolation phase.

In the next section, we will discuss the results obtained in the trapping region.

4.3. Trapping regime

In this region, we are interested to study the final positions (X_f, Y_f) of trapped particles depending on the characteristics of the disk packing. To this end, we record X_f and Y_f once the particle was trapped and as b is changed from b_c to 1, until

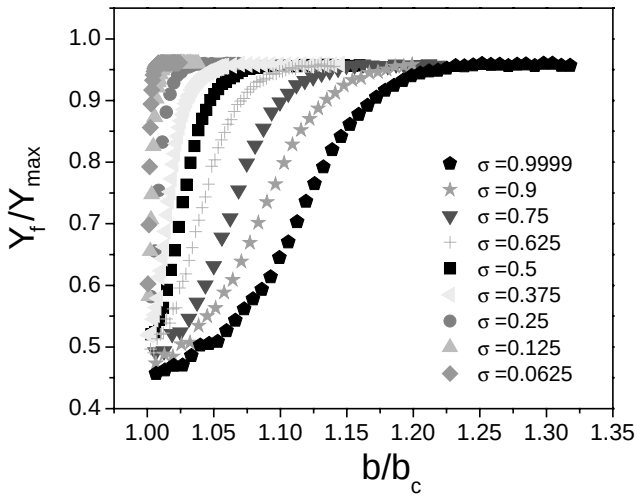

Fig. 14. Relative final vertical position of the trapped particle as a function of adimensional b/b_c. Y_{max} is the maximum height of the array of disks once the pouring is finished.

saturation. We cover the whole range of possible values for σ. In Fig. 14, we plot the relative final vertical position of the trapped particle as a function of adimensional b/b_c. Y_{max} is the maximum height of the array of disks once the pouring is finished. Two main features can be observed from the figure. First, the limiting values of relative height Y_f/Y_{max} for great values of b (far from percolation) are practically independent of the dispersion of disks. This means that the penetration percentages of the small particle in dispersed mixtures of grains is similar to that for monosized ones.

Secondly, the widespread of the final vertical positions is strongly dependent on σ as b departures from b_c. For small σ we practically found a step-like function. We have already pointed out this fact when analyzed the X distributions of the trapped particle in Figs. 8 and 9. For small σ, the transition is practically abrupt, given the fact that allowed paths are proportional to $R(1-b)$ and the radii distribution is practically a delta function. For the extreme case $\sigma=0$, the Y distribution would be a step function.

Let us keep in mind that smaller b values correspond to a looser disk packing. So, when you want to mix small particles in a matrix of larger ones whose radii distribution has a dispersion σ, a procedure to loosen the packing will produce a better vertical distribution of the percolating grains for the case of great dispersion than for the case of poor dispersed assemblies. In other words, for small σ, a short range of b values can be used in order to generate the mixture.

In Fig. 15, we show typical results for the probability distribution of the final horizontal position (X_f) for the percolating particle for the case of $\sigma=0.9$. All results are averaged over 2×10^3 equivalent realizations. We observe a uniformly distribution for the probability, different from the peek behavior in Figs. 7–9. This is due to the fact that the launching point in these simulations was taken at random over the top of the array of disks, imaging a "hole" of 1/3 the width of the die, at the middle of it, while

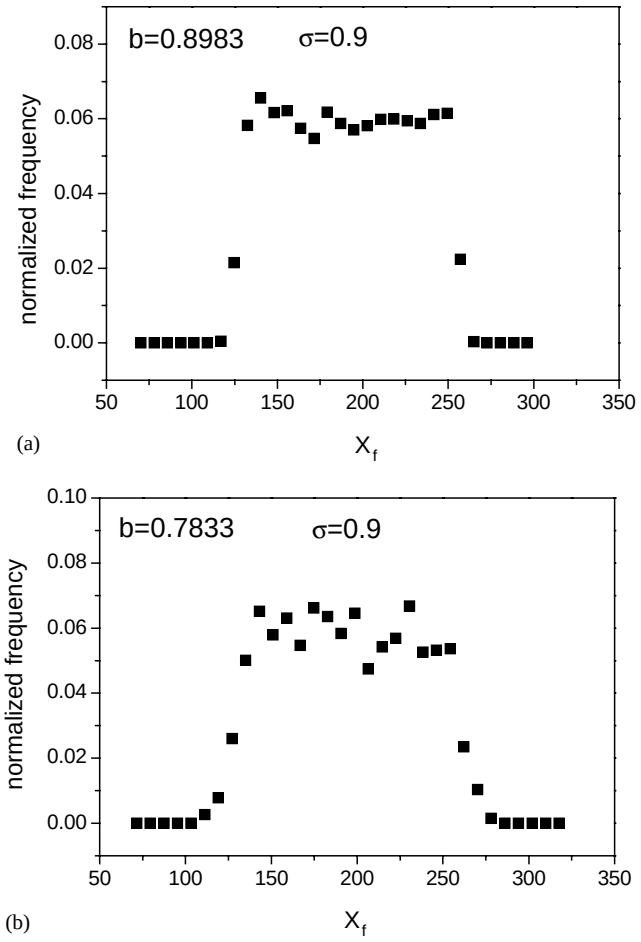

Fig. 15. (a,b) Typical results for the probability distribution of the final horizontal position (X_f) for the percolating particle when $\sigma = 0.9$. (here $b_c = 0.7783$).

in the cases above, it was fixed at the middle of the die. This difference is important when one wants to select the technique for pouring the small grains, depending on the desired mixture characteristics. The width of the distributions is practically insensitive to σ and b, presenting a small increase in dispersivity for b close to b_c, as can be appreciated comparing Fig. 15(a) with (b). Remember that $b_c = 0.7783$ for $\sigma = 0.9$.

5. Conclusions

In this paper, we presented a simulation algorithm to generate 2-D random packings of disks whose radii size distribution can be, in principle, of any desired shape. Given

the wide range of applications that this kind of granular media modeling may represent, we wanted to characterize, in some extent, static and dynamical features of these packed grains systems. To this end, we measured contact force and displacement distributions (static aspects) and percolation of small particles (dynamic aspect) on thousands of similar samples of these packings.

Concerning the first aspect, we found previously, and use here, that our system is isostatic and this property allows us to easily calculate the desired distributions of forces and displacements [21,22,25,26].

A low-frequency high-amplitude relaxation process was performed after each packing was generated. This relaxation process was useful to rearrange the disks in the packing, lowering considerably the number of bridges. It practically does not affect the density of the system and does not cause considerable segregation [26], but its main effect was to enhance the stability of the system. This is shown by the lower rate of negative to positive forces as relaxations go further.

Forces and displacements have broad distributions. They are power law functions of the strength and have a cutoff value which grows exponentially with depth or height, respectively. This similar behavior in both kind of distributions supports the original idea that, if no sign constraints exists for stresses, power law behavior is expected in isostatic systems. For the case of monosized distributions of radii, we recovered previously reported results [25].

We may say that relaxations produce a redistribution of stresses and displacements, lowering their strength. This is not a steric effect, nor a topologic one, but seems to be a scaling effect closely related to ordering the system. We have to investigate these conjectures deeply with further simulations.

It would be interesting to look for the universal behavior of these structures through a systematic study of the exponents implied in the power law behavior found. On the other hand, introduction of friction will increase the number of bridges and will affect the stress distributions.

Concerning dynamical features, we may say that this is the first time (to our present knowledge) that the dependence of a percolation parameter (like b_c) is found as a function of a packing distribution parameter (σ) in a granular assembly, and a power law dependence has been found out.

For small dispersion values, the system presents an abrupt transition from non-percolative to percolative regimes, i.e., the particles soon get trapped, with almost no penetration at all. The dynamics of the diffusing process that no longer belongs to a standard one. For greater values of σ, the transition smoothes. This can be appreciated clearly in Figs. 10 and 11. In the non-trapping regime, we always found a Gaussian-like exit distribution for all values of σ studied, resembling experiments [11].

Successive Y_p positions of the small falling particle show that, in the non-trapping regime, it "sees" the same effective medium as it falls down. This is proved in Figs. 12 and 13. In the trapping regime, as b departures from b_c, the slopes are steeper. This is due to the existence of a few number of possible ways to percolate, thus, the falling down (if could happen) gets more effective.

In the trapping regime, the strong dependence of Y_f on σ, as b departures from b_c, and the sensibility of X_f on the pouring method, allow to conclude that a procedure to

loosen the packing will produce a better vertical distribution of the percolating grains for the case of great packed particles dispersion than for the case of poor dispersed assemblies. In other words, for small σ, a short range of b values can be used in order to generate the mixture.

Conclusions above help to select appropriate experimental techniques, depending on how are the desired mixture characteristics. They tell us how to pour small grains and how to shake our packed particles taking into account the final distributions of small particles and forces among grains we are looking for.

Given the advantages of the present algorithm concerning CPU time and size distribution possibilities, a wide variety of experimental setups can be simulated in order to predict interesting properties of packed grains in other systems of technological and basic interest. Present efforts are driven in this direction.

References

[1] H.J. Herrmann, J.P. Hovi, S. Luding, Physics of Dry Granular Media, Kluwer Academic Publisher, Dordrecht, 1998, pp. 137, 197, 319, 633 among others.
[2] V.M. Kenkre, M.R. Endicott, S.J. Glass, A.J. Hurd, J. Am. Ceram. Soc. 79 (1996) 3045.
[3] R. Kamm, M.A. Steinberg, J. Wulff, Trans. Amer. Inst. Mech. Eng. 171 (1947) 439.
[4] R.P. Seeling, Trans. Amer. Inst. Mech. Eng. 171 (1947) 506.
[5] R.A. Thompson, Ceram. Bull. 60 (1981) 237.
[6] J. Bridgwater, W. Sharpe, D.C. Stocker, Trans. Inst. Chem. Eng. 47 (1969) 114.
[7] J. Bridgwater, M.H.C. Cooke, A.M. Scott, Trans. Inst. Chem. Eng. 56 (1978) 157.
[8] M.H.C. Cooke, J. Bridgwater, Indus. Eng. Chem. Fundam. 18 (1979) 25.
[9] P. Meaking, R. Jullien, J. Phys. France 51 (1990) 2673.
[10] J. Bridgwater, D. Ingram, Trans. Inst. Chem. Eng. 49 (1971) 163.
[11] I. Ippolito, L. Samson, S. Bourles, J.P. Hulin, Eur. Phys. J.E 3 (2000) 227.
[12] G.T. Nolan, P.E. Kavanagh, Powder Technol. 72 (1992) 149;
G.T. Nolan, P.E. Kavanagh, Powder Technol. 76 (1993) 301;
G.T. Nolan, P.E. Kavanagh, Powder Technol. 78 (1994) 231.
[13] J. Grindlay, A.H. Opie, Phys. Rev. E 51 (1995) 718.
[14] S. Luding, Phys. Rev. E 55 (1997) 4720.
[15] D.C. Hong, Phys. Rev. E 47 (1993) 760.
[16] F. Radjai, D.E. Wolf, M. Jean, J.J. Moreau, Phys. Rev. Lett. 80 (1998) 61.
[17] S.F. Edwards, D.V. Grinev, Phys. Rev. Lett. 82 (1999) 5397.
[18] H. Herrmann, S. Luiding, Continuum Mech. Thermodyn. 10 (1998) 189.
[19] S. Ouaguenouni, J. Roux, Europhys. Lett. 32 (1995) 449;
S. Ouaguenouni, J. Roux, Europhys. Lett. 39 (1997) 117.
[20] F. Radjai, J. Schafer, S. Dippel, D. Wolf, J. Phys. I 7 (1997) 1053.
[21] C.F. Moukarzel, Phys. Rev. Lett. 81 (1998) 1634, and references therein.
[22] C.F. Moukarzel, Rigidity theory, and applications, Fundamental Material Science, Plenum Press, New York, 1999, pp. 125.
[23] R. Jullien, P. Meakin, A. Pavlovitch, Phys. Rev. Lett. 69 (1992) 640.
[24] F. Radjai, S. Roux, J.J. Moreau, Chaos 9 (1999) 544.
[25] C. F. Moukarzel, Granular Matter 3 (2001) 41.
[26] A.M. Vidales, V.M. Kenkre, A. Hurd, Granular Matter 3 (2001) 141.
[27] A. Tkachenko, T. Witten, Phys. Rev. E 60 (1999) 687.
[28] A. Tkachenko, T. Witten, Phys. Rev. E 62 (2000) 2510.
[29] L. Bruno, Difusión y mezcla en medios granulares, Ph.D. Thesis, Universidad de Buenos Aires, 2002.